

Quantum Resistor-Capacitor Circuit with Majorana Fermion Modes in Chiral Topological Superconductor: Supplementary Material

Minchul Lee¹ and Mahn-Soo Choi²

*¹Department of Applied Physics, College of Applied Science,
Kyung Hee University, Yongin 446-701, Korea*

²Department of Physics, Korea University, Seoul 136-701, Korea

In this Supplementary Material we comments on the build-up of our model Hamiltonian and provide the detailed derivation and analysis of the linear-response admittance and the corresponding relaxation resistance. We also compare in detail the Majorana modes and the ordinary Andreev bound states.

CONTENTS

I. Model Hamiltonians	2
II. Linear-Response Admittance and Relaxation Resistance	3
A. Self-consistent Linear-Response Theory	3
B. Green's Function and Admittance	4
C. Relaxation Resistance at Zero Temperature	7
D. All-Majorana Representation	8
E. Relaxation Resistance at Finite Temperatures: Sommerfeld Expansion	10
III. Comparison with the Case with Andreev Edge Modes	11
A. Andreev Edge Modes: Conventional Andreev Edge Mode vs. Majorana Mode	11
B. Model for Conventional Andreev Edge Mode	12
C. Linear Response Theory	13
D. Relaxation Resistance: Below the Superconducting Gap	14
E. Relaxation Resistance: Above the Superconducting Gap	15
F. Summary of Differences between <i>s</i> -wave Andreev Edge Mode and Majorana Mode	16
References	18

I. MODEL HAMILTONIANS

The Hamiltonian for the Majorana edge modes is constructed based on that of the Dirac fermion edge mode as given in Eq. (6) in the main text. In the absence of superconductivity, the Hamiltonian (6) is that for the QAH edge mode. Via the relation $c_k = (\gamma_{k,1} + i\gamma_{k,2})/2$, or inversely

$$\gamma_{k,1} = \frac{c_k + c_{-k}^\dagger}{\sqrt{2}} \quad \text{and} \quad \gamma_{k,2} = \frac{c_k - c_{-k}^\dagger}{\sqrt{2}i}, \quad (\text{S1})$$

the Dirac fermion Hamiltonian (6) turns into the Majorana fermion Hamiltonian (1). Proximity-coupled to a *s*-wave superconductor, two Majorana fermion modes are spatially separated. However, they are still degenerate in energy [1]. Therefore, the Hamiltonians (6) and (7) are valid in the cTSC₂ phase. In the cTSC₁ phase, the $j = 2$ Majorana mode becomes gapped so that it is missing. In our study, the disappearance of $j = 2$ mode is accounted for by turning off its coupling to the dot: $t_2 = 0$, see below.

The build-up of the tunneling Hamiltonian between the Majorana fermion modes and the dot electron starts with the fermionic coupling Hamiltonian which couples the QAH edge modes and the dot electron:

$$H_{\text{tun}}^{\text{QAH}} = \sum_k \left[t_k d^\dagger c_k + (\text{h.c.}) \right], \quad (\text{S2})$$

where t_k is the momentum-dependent tunneling amplitude. In terms of the MF operators, it reads

$$H_{\text{tun}}^{\text{QAH}} = \sum_k \frac{1}{\sqrt{2}} \left[t_k d^\dagger \gamma_{k,1} + i t_k d^\dagger \gamma_{k,2} + (\text{h.c.}) \right]. \quad (\text{S3})$$

Upon the proximity-induced superconductivity, the overlaps between the Majorana modes and the dot electron become different for $j = 1, 2$ due to the different spatial localization of the Majorana modes [1]. So t_k now has the j -dependence, $t_{k,j}$ [2] so that one obtains the tunneling Hamiltonian (3) with $|t_{1,k}| > |t_{2,k}|$. In terms of the Dirac fermion operator and dropping the k -dependence, the tunneling Hamiltonian is rewritten as Eq. (7), in which the pairing term, missing in the original QAH edge Hamiltonian, appears. Hence the pairing term, whose amplitude is $t_{\text{pair}} = (t_1 - t_2)/\sqrt{2}$, is due to the mismatch in the coupling of the dot electron to two Majorana modes.

II. LINEAR-RESPONSE ADMITTANCE AND RELAXATION RESISTANCE

A. Self-consistent Linear-Response Theory

We consider a nanoscale capacitor (quantum dot) coupled to the Majorana fermion reservoir. A weak time-dependent external gate voltage $V_g(t) = V_{\text{ac}} \cos \omega t$ is applied on the quantum dot. In such a coherent RC circuit, the AC transport is highly sensitive to the internal distribution of charges and potentials, which needs to be calculated in a self-consistent manner to ensure the gauge invariance and current conservation [3–7]. In the mean-field approximation, the time-dependent voltage $V_g(t)$ induces the polarization charges $N_U(t)$ between the dot and the gate, which in turn leads to the time-dependent potential $U(t) = |e|N_U(t)/C$ inside the dot. Consequently, the applied voltage not only generates a current $I(t)$ between the lead and the dot, but also induces a dot-gate displacement current $I_d(t) = e(dN_U/dt) = -C(dU/dt)$. Charge conservation requires $I(t) + I_d(t) = 0$. Assuming that the gate-invariant perturbation, $V_g(t) - U(t)$, is sufficiently small, the linear response theory leads to the relation, $I(\omega) = g(\omega)(V_g(\omega) - U(\omega))$, where $g(t) = (ie/\hbar) \langle [I(t), n_d] \rangle \Theta(t)$ is the equilibrium correlation function between the occupation operator $n_d = d^\dagger d$ and the current operator $I = e(dn_d/dt)$. Note that the current-density correlation function $g(\omega)$ is directly related to the charge susceptibility $\chi_c(t) = -i \langle [n_d(t), n_d] \rangle \Theta(t)$, via the relation $g(\omega) = i\omega(e^2/\hbar)\chi_c(\omega)$. Then, with the help of $I(\omega) = -I_d(\omega) = -i\omega C U(\omega)$, the dot-lead impedance $Z(\omega) = V_g(\omega)/I(\omega)$, which is experimentally accessible, is given by $Z(\omega) = 1/(-i\omega C) + 1/g(\omega)$. Then, the

relaxation resistance and the quantum correction to the capacitance is obtained by $1/g(\omega) = R_q(\omega) + i/\omega C_q(\omega)$. Explicitly, the relaxation resistance is given by

$$R_q(\omega) = \text{Re} \left[\frac{1}{g(\omega)} \right] = \frac{\text{Re}[g(\omega)]}{\text{Re}[g(\omega)]^2 + \text{Im}[g(\omega)]^2}. \quad (\text{S4})$$

In the low-frequency limit, usually $|\text{Re}[g(\omega)]| \ll |\text{Im}[g(\omega)]|$ (since $\text{Im}[g(\omega)] \propto \omega$ and $\text{Re}[g(\omega)] \propto \omega^2$) so that

$$R_q(\omega) \approx \frac{\text{Re}[g(\omega)]}{\text{Im}[g(\omega)]^2}, \quad (\text{S5})$$

which means that the low-frequency relaxation resistance is proportional to the real part of the admittance. Accordingly, we have examined $\text{Re}[g(\omega)]$ in the main text in order to estimate the amplitude of the dissipation.

B. Green's Function and Admittance

While the admittance can be obtained in terms of the charge susceptibility, we instead follow the Wingreen-Meir formalism [8, 9] which derives directly the current formula for arbitrary gauge-invariant perturbation $V_g(t) - U(t)$ and then obtains the admittance by considering the linear response only. Before following the formalism, it is convenient to apply a gauge transformation which transfers the time-dependence from the QD Hamiltonian to the tunneling Hamiltonian. Under the time-dependent unitary transformation $U = \exp[\frac{i}{\hbar}S(t)]$ defined as

$$S(t) = \int^t dt' e(U(t') - V_g(t'))n_d, \quad (\text{S6})$$

the Hamiltonian is transformed into

$$H = H_{\text{Majorana}} + H_{\text{QD}} + H_{\text{tun}}(t). \quad (\text{S7})$$

Here H_{Majorana} is unchanged, $H_{\text{QD}} = \epsilon_d n_d$, and

$$H_{\text{tun}} = \sum_k \left[t_1(t) d^\dagger \gamma_{k,1} + i t_2(t) d^\dagger \gamma_{k,2} + (\text{h.c.}) \right] \quad (\text{S8})$$

with $t_j(t) = t_j e^{i\Delta(t)}$ and

$$\Delta(t) \equiv \frac{i}{\hbar} \int^t dt' e(U(t') - V_g(t')). \quad (\text{S9})$$

Based on the gauge-transformed Hamiltonian, it is quite straightforward to setup non-equilibrium Green's functions and Dyson equations for them. Since the Majorana fermion comes from the superconductivity, it is useful to express the Green's function in Nambu space. The retarded/advanced/lesser QD

Green's functions are then written as

$$G_d^{R/A}(t, t') = \mp i \Theta(\pm(t - t')) \begin{bmatrix} \langle |\{d(t), d^\dagger(t')\} \rangle & \langle |\{d(t), d(t')\} \rangle \\ \langle |\{d^\dagger(t), d^\dagger(t')\} \rangle & \langle |\{d^\dagger(t), d(t')\} \rangle \end{bmatrix} \quad (\text{S10a})$$

$$G_d^<(t, t') = i \begin{bmatrix} \langle |d^\dagger(t')d(t)| \rangle & \langle |d(t')d(t)| \rangle \\ \langle |d^\dagger(t')d^\dagger(t)| \rangle & \langle |d(t')d^\dagger(t)| \rangle \end{bmatrix} \quad (\text{S10b})$$

and their Dyson's equations are found to be

$$G_d^{R/A}(t, t') = g_d^{R/A}(t - t') + \int dt'' \int dt''' g_d^{R/A}(t - t'') \Sigma^{R/A}(t'', t''') G_d^{R/A}(t''', t') \quad (\text{S11a})$$

$$G_d^<(t, t') = \int dt'' \int dt''' G_d^R(t, t'') \Sigma^<(t'', t''') G_d^A(t''', t'). \quad (\text{S11b})$$

Here $\Sigma^{R/A/<}(t, t')$ are the self energies defined as

$$\Sigma^{R/A/<}(t, t') \equiv \sum_k \frac{M^\dagger(t)}{\hbar} g_k^{R/A/<}(t - t') \frac{M(t')}{\hbar}. \quad (\text{S12})$$

The QD-Majorana coupling matrix $M(t)$ in the Nambu space is given by

$$M(t) \equiv \begin{bmatrix} t_{\text{single}}^* & -t_{\text{pair}} \\ t_{\text{pair}}^* & -t_{\text{single}} \end{bmatrix} e^{-i\Delta(t)\sigma_3} \quad (\text{S13})$$

and $g_d^{R/A/<}(t)$ and $g_k^{R/A/<}(t)$ are unperturbed equilibrium retarded/advanced/lesser QD and Dirac fermion

Green's functions which are expressed in the frequency domain as

$$g_d^{R/A}(\omega') = \frac{1}{\omega' - \sigma_3 \epsilon_d / \hbar \pm i0^+}, \quad g_d^<(\omega') = 2\pi f(\hbar\omega') \delta(\omega' - \sigma_3 \epsilon_d / \hbar), \quad (\text{S14a})$$

$$g_k^{R/A}(\omega') = \frac{1}{\omega' - \sigma_3 \epsilon_k / \hbar \pm i0^+}, \quad g_k^<(\omega') = 2\pi f(\hbar\omega') \delta(\omega' - \sigma_3 \epsilon_k / \hbar), \quad (\text{S14b})$$

respectively. Here $f(\epsilon)$ is the Fermi distribution function at temperature T . In the absence of the AC driving ($\Delta(t) = 0$), the Dyson's equations lead to the equilibrium QD Green's functions

$$G_d^{R/A}(\omega') = \left[g_d^{R/A}(\omega') - \Sigma^{R/A}(\omega') \right]^{-1} \quad \text{and} \quad G_d^<(\omega') = G_d^R(\omega') \Sigma^<(\omega') G_d^A(\omega') \quad (\text{S15})$$

with the equilibrium self energies given by

$$\Sigma^{R/A}(\omega') = \mp \frac{i}{2} \begin{bmatrix} \Gamma_+ & \Gamma_- \\ \Gamma_- & \Gamma_+ \end{bmatrix} \quad \text{and} \quad \Sigma^<(\omega') = i f(\hbar\omega') \begin{bmatrix} \Gamma_+ & \Gamma_- \\ \Gamma_- & \Gamma_+ \end{bmatrix}, \quad (\text{S16})$$

where Γ_\pm is as defined in the main text. The explicit form of the equilibrium retarded/advanced Green's functions in Eq. (S15) are given by

$$G_d^{R/A}(\omega) = \left[\begin{array}{cc} \omega - \epsilon_d \pm i \frac{\Gamma_\pm}{2} & \pm i \frac{\Gamma_\mp}{2} \\ \pm i \frac{\Gamma_\mp}{2} & \omega + \epsilon_d \pm i \frac{\Gamma_\pm}{2} \end{array} \right]^{-1}. \quad (\text{S17})$$

In the presence of small AC driving, suppose that $V_g(t) - U(t) \equiv V_{ac} \cos \omega t$ and accordingly,

$$\Delta(t) = -\frac{eV_{ac}}{\hbar\omega} \sin \omega t \equiv v \sin \omega t. \quad (\text{S18})$$

Up to the linear order in v , the non-equilibrium QD Green's functions are expanded as

$$\begin{aligned} G_d^{R/A}(\omega', \omega'') &= \frac{1}{2\pi} \int dt' \int dt'' e^{i(\omega't' - \omega''t'')} G_d^{R/A}(t', t'') \\ &= G_d^{R/A}(\omega') \delta(\omega' - \omega'') + \frac{v}{2} \left((1 + \omega G_d^{R/A}(\omega')) \sigma_3 G_d^{R/A}(\omega' + \omega) - G_d^{R/A}(\omega') \sigma_3 \right) \delta(\omega' - \omega'' + \omega) \\ &\quad - \frac{v}{2} \left((1 - \omega G_d^{R/A}(\omega')) \sigma_3 G_d^{R/A}(\omega' - \omega) - G_d^{R/A}(\omega') \sigma_3 \right) \delta(\omega' - \omega'' - \omega) \end{aligned} \quad (\text{S19a})$$

$$\begin{aligned} G_d^<(t, t') &= \int \frac{d\omega'}{2\pi} e^{i\omega'(t'-t)} \left[G_d^R(\omega') \Sigma^<(\omega') G_d^A(\omega') \right. \\ &\quad + \frac{v}{2} \left(e^{+i\omega t} (1 + \omega G_d^R(\omega' - \omega)) - e^{-i\omega t} (1 - \omega G_d^R(\omega' + \omega)) \right) \sigma_3 G_d^R(\omega') \Sigma^<(\omega') G_d^A(\omega') \\ &\quad \left. + \frac{v}{2} G_d^R(\omega') \Sigma^<(\omega') G_d^A(\omega') \sigma_3 \left(e^{-i\omega t'} (1 + \omega G_d^A(\omega' - \omega)) - e^{+i\omega t'} (1 - \omega G_d^A(\omega' + \omega)) \right) \right]. \end{aligned} \quad (\text{S19b})$$

For later use, we also need to define the QD-Dirac fermion Green's functions $G_{d,k}^{</>t/\bar{t}}$ similarly to the QD Green's functions: For example,

$$G_{d,k}^<(t, t') = i \begin{bmatrix} \langle |c_k^\dagger(t') d(t)| \rangle & \langle |c_k(t') d(t)| \rangle \\ \langle |c_k^\dagger(t') d^\dagger(t)| \rangle & \langle |c_k(t') d^\dagger(t)| \rangle \end{bmatrix} \quad (\text{S20})$$

and

$$G_{d,k}^t(t, t') = -i \begin{bmatrix} \langle |\mathcal{T}_c d(t) c_k^\dagger(t')| \rangle & \langle |\mathcal{T}_c d(t) c_k(t')| \rangle \\ \langle |\mathcal{T}_c d^\dagger(t) c_k^\dagger(t')| \rangle & \langle |\mathcal{T}_c d^\dagger(t) c_k(t')| \rangle \end{bmatrix}. \quad (\text{S21})$$

The equation-of-motion method relates the QD-Dirac fermion Green's functions to the QD Green's functions via the following Dyson's equations:

$$\widehat{G}_{d,k}(t, t') = \int dt'' \widehat{G}_d(t, t'') \frac{M^\dagger(t'')}{\hbar} \tau_3 \widehat{g}_k(t'', t'), \quad (\text{S22})$$

where \widehat{g}_k , \widehat{G}_d and so on are the matrix forms of the Green's functions such as

$$\widehat{g}_k \equiv \begin{bmatrix} g_k^t & g_k^< \\ g_k^> & g_k^{\bar{t}} \end{bmatrix} \quad \text{and} \quad \widehat{G}_d \equiv \begin{bmatrix} G_d^t & G_d^< \\ G_d^> & G_d^{\bar{t}} \end{bmatrix} \quad (\text{S23})$$

and τ_3 are the Pauli matrix in the Keldysh space.

Now we are ready to express the current $I(t)$ in terms of the QD Green's functions. The current, being the expectation value of the current operator $e(dn_d/dt)$, is expressed as

$$I(t) = e \left\langle \frac{dn_d}{dt} \right\rangle = \frac{ie}{\hbar} \sum_k \left[t_{\text{single}}^*(t) \langle |c_k^\dagger(t) d(t)| \rangle + t_{\text{pair}}^*(t) \langle |c_k(t) d(t)| \rangle - (\text{h.c.}) \right] = \frac{2e}{\hbar} \text{Re} \sum_k \left[G_{d,k}^<(t) M(t) \right]_{11}. \quad (\text{S24})$$

Using the Dyson's equation, Eq. (S22), the current can be written solely in terms of the QD Green's function:

$$I(t) = 2e \operatorname{Re} \int dt' [G_d^R(t, t')\Sigma^<(t', t) + G_d^<(t, t')\Sigma^A(t', t)]_{11}. \quad (\text{S25})$$

By substituting the linearized QD Green's functions, Eq. (S19) into the current formula and performing a tedious arrangement, the linear-response current with respect to the AC signal with frequency ω , Eq. (S18) is obtained by

$$I(\omega) = \frac{ev\omega^2}{2\pi} \int d\omega' f(\hbar\omega') [G_d^R(\omega' - \omega)\sigma_3(G_d^R(\omega') - G_d^A(\omega')) + (G_d^R(\omega') - G_d^A(\omega'))\sigma_3G_d^A(\omega' + \omega)]_{11}. \quad (\text{S26})$$

In obtaining the above formula one has to use the following relations in equilibrium:

$$\begin{aligned} G_d^R(\omega)\Sigma^<(\omega)G_d^A(\omega) &= f(\hbar\omega)(G_d^A(\omega) - G_d^R(\omega)), \quad \Sigma^<(\omega) = -f(\epsilon)(\Sigma^R(\omega) - \Sigma^A(\omega)), \\ \text{and } g_d^{-1}G_d^{R/A} - \Sigma^{R/A}G_d^{R/A} &= G_d^{R/A}g_d^{-1} - G_d^{R/A}\Sigma^{R/A} = 1. \end{aligned} \quad (\text{S27})$$

Hence we arrive at the admittance $g(\omega) = I(\omega)/V_{\text{ac}}$ given by

$$g(\omega) = \frac{\omega}{R_Q} \int d\omega' f(\omega') [G_d^R(\omega' - \omega)\sigma_3\{G_d^R(\omega') - G_d^A(\omega')\} + \{G_d^R(\omega') - G_d^A(\omega')\}\sigma_3G_d^A(\omega' + \omega)]_{11}. \quad (\text{S28})$$

C. Relaxation Resistance at Zero Temperature

While the finite-temperature admittance is numerically calculated by directly using Eq. (S28), the zero-temperature admittance allows the closed-form expression as given in Eq. (4) in the main text, by using the integral

$$\int_{-\infty}^0 \frac{dx}{x + a + ib} = \ln \frac{|b| - i(\operatorname{sgn} b)a}{|b| - i(\operatorname{sgn} b)(-\infty)}. \quad (\text{S29})$$

The zero-frequency relaxation resistance can be obtained by taking the $\omega \rightarrow 0$ limit:

$$R_0 = \frac{R_Q}{2} \frac{\Gamma_1\Gamma_2}{\Gamma_+^2} \left(\frac{(\epsilon/2)^2}{(\epsilon_d/\hbar)^2 - ((2\epsilon_d/\hbar)^2 + \Gamma_1\Gamma_2)\Gamma_c/8\Gamma_+} \right)^2 \quad (\text{S30})$$

with

$$\Gamma_c \equiv \frac{i\Gamma_-^2}{\epsilon} \ln \frac{\Gamma_+ - i\epsilon}{\Gamma_+ + i\epsilon} \quad \text{and} \quad \epsilon \equiv \sqrt{(2\epsilon_d/\hbar)^2 - \Gamma_-^2}. \quad (\text{S31})$$

Note that Γ_c is always real. The weak-coupling value of the resistance, Eq. (5) can be readily obtained by taking the limit $|\epsilon_d/\hbar| \gg \Gamma_1$ in Eq. (S30).

Two important features of the zero-frequency resistance should be remarked here. First, the zero-frequency resistance, Eq. (S30) vanishes exactly, $R_0 = 0$ if the $j = 2$ Majorana mode is detached ($\Gamma_2 = 0$), irrespective of the QD level and the transmission of the tunneling barrier. Second, near the resonance ($|\epsilon_d| \ll \Gamma_1$), R_0 , as a function of Γ_2 , has a local maximum in the interval $0 < \Gamma_2 < \Gamma_1$. The maximum occurs at $\Gamma_2 \approx \Gamma_m \equiv 4\epsilon_d^2/\Gamma_1$, and its height scales as $\sim [4\gamma_m \ln \gamma_m]^{-1}$ with $\gamma_m \equiv \Gamma_m/\Gamma_1$. Hence, as the resonance comes closer, the maximum of the resistance diverges.

Now consider the finite-frequency resistance in the $cTSC_1$ phase ($\Gamma_2 = 0$). Since $R_0 = 0$ in this phase, the leading-order term of the low-frequency resistance with respect to the frequency should be of the second order in ω . Explicitly,

$$R_q(\omega) = \frac{R_Q}{3} \left(\frac{(\epsilon_d/\hbar)^2 - (\Gamma_1/4)^2}{(\epsilon_d/\hbar)^3 \left(1 - \frac{\Gamma_1}{4} \frac{i}{\epsilon} \ln \frac{\Gamma_1/2 - i\epsilon}{\Gamma_1/2 + i\epsilon} \right)} \right)^2 \omega^2 + \mathcal{O}(\omega^4). \quad (\text{S32})$$

Equations (8) and (9) in the main text can be obtained by taking the limits $|\epsilon_d/\hbar| \gg \Gamma_1$ and $|\epsilon_d/\hbar| \ll \Gamma_1$, respectively.

Interesting finite-frequency behavior arises at the resonance ($\epsilon_d = 0$). In this condition, the $j = 1$ and $j = 2$ Majorana modes 1 and 2 are completely decoupled as discussed in the main text and below. However, two modes still interfere with each other in the electron transport, as can be seen in the expression of the admittance:

$$g(\omega) = \frac{-i\omega}{R_Q} \left(\frac{\Gamma_1}{\omega^2 - i\Gamma_2\omega - \Gamma_+\Gamma_-} \ln \frac{\Gamma_2 + i(2\omega)}{\Gamma_2} + \frac{\Gamma_2}{\omega^2 - i\Gamma_1\omega + \Gamma_+\Gamma_-} \ln \frac{\Gamma_1 + i(2\omega)}{\Gamma_1} - \frac{2\Gamma_-}{\Gamma_-^2 + \omega^2} \ln \frac{\Gamma_2}{\Gamma_1} \right). \quad (\text{S33})$$

In the $cTSC_1$ phase, the finite-frequency resistance is then obtained by setting $\Gamma_2 = 0$ so that

$$R_q(\omega) = R_Q \frac{\omega^2 + (\Gamma_1/2)^2}{\Gamma_1|\omega|} \frac{\pi/2}{(\pi/2)^2 + (\ln(2|\omega|/\Gamma_1))^2} \quad (\text{S34})$$

which is approximated as Eq. (10) in the $\omega \rightarrow 0$ limit. Therefore, it exhibits a divergence at zero frequency.

D. All-Majorana Representation

As proposed in the main text, all the fermion operators in the Hamiltonian, including the QD electron operator, can be, at least mathematically, decomposed into the Majorana fermion operators. Defining two QD Majorana operators $\gamma_{d,j}$ ($j = 1, 2$) by $\gamma_{d,1} = (d - d^\dagger)/\sqrt{2}i$ and $\gamma_{d,2} = (d + d^\dagger)/\sqrt{2}$, the QD and

tunneling Hamiltonians are rewritten as

$$H_{\text{QD}} = i(\epsilon_d + e(U(t) - V_g(t))\gamma_{d,2}\gamma_{d,1}) \quad (\text{S35a})$$

$$H_{\text{tun}} = \sum_k i(t_2\gamma_{d,2}\gamma_{k,2} - t_1\gamma_{d,1}\gamma_{k,1}), \quad (\text{S35b})$$

respectively. These equations become Eq. (11) in the main text in the DC limit ($V_g(t) = U(t) = 0$). In deriving the above Hamiltonians, we assume that the tunneling amplitudes are real: $t_j = t_j^*$, which can be always satisfied via a proper gauge transformation. Applying the time-dependent unitary transformation $U = \exp[\frac{i}{\hbar}S(t)]$ as defined in Eq. (S6), the time-dependence moves into the tunneling Hamiltonian so that we have

$$H_{\text{QD}} = i\epsilon_d\gamma_{d,2}\gamma_{d,1} \quad (\text{S36a})$$

$$H_{\text{tun}} = \sum_k i[-t_1 \cos \Delta(t)\gamma_{d,1}\gamma_{k,1} + t_1 \sin \Delta(t)\gamma_{d,2}\gamma_{k,1} + t_2 \sin \Delta(t)\gamma_{d,1}\gamma_{k,2} + t_2 \cos \Delta(t)\gamma_{d,2}\gamma_{k,2}]. \quad (\text{S36b})$$

It should be noted that in the DC limit the $j = 1$ and $j = 2$ Majorana modes are completely decoupled at the resonant condition ($\epsilon_d = 0$). However, the gauge-transformed Hamiltonian (S36) shows that a finite ac driving effectively couples the $j = 1$ and $j = 2$ Majorana modes even if the dot level is zero ($\epsilon_d = 0$). This is the reason why the two Majorana modes interfere with each other in the electron transport even at resonance (see Eq. (S33)).

Now we follow the procedure of the linear-response theory as done in Sec. 2B by redefining the QD Green's function in terms of the Majorana fermion operators:

$$G_{d,M}^{R/A}(t, t') = \mp i\Theta(\pm(t - t')) \begin{bmatrix} \langle |\{\gamma_{d,1}(t), \gamma_{d,1}(t')\}| \rangle & \langle |\{\gamma_{d,1}(t), \gamma_{d,2}(t')\}| \rangle \\ \langle |\{\gamma_{d,2}(t), \gamma_{d,1}(t')\}| \rangle & \langle |\{\gamma_{d,2}(t), \gamma_{d,2}(t')\}| \rangle \end{bmatrix}. \quad (\text{S37})$$

In fact, the forms of the Dyson's equations for Majorana Green's functions are identical to those in Sec. 2B except that all the Green's functions are properly replaced by the Majorana-based ones. Finally we then obtain the admittance

$$g(\omega) = \frac{\omega}{R_Q} \int d\omega' f(\omega') \text{tr} \left\{ [G_{d,M}^R(\omega' - \omega)\sigma_2\{G_{d,M}^R(\omega') - G_{d,M}^A(\omega')\} + \{G_{d,M}^R(\omega') - G_{d,M}^A(\omega')\}\sigma_2 G_{d,M}^A(\omega' + \omega)] \frac{\sigma_0 + \sigma_2}{2} \right\}. \quad (\text{S38})$$

Here the appearance of additional Pauli matrices is owing to the unitary transformation from the QD fermion operator to the Majorana fermion operator. The equilibrium retarded/advanced QD Green's functions are

given by

$$G_{d,M}^{R/A} = \left([g_{d,M}^{R/A}(\omega)]^{-1} - \Sigma^{R/A}(\omega) \right)^{-1} = \begin{bmatrix} \omega \pm i\frac{\Gamma_1}{2} & -i\epsilon_d/\hbar \\ i\epsilon_d/\hbar & \omega \pm i\frac{\Gamma_2}{2} \end{bmatrix}^{-1}. \quad (\text{S39})$$

The Green's functions, whose off-diagonal components vanish at $\epsilon_d = 0$, reflect that the two modes are decoupled at resonance. The real and imaginary parts of the diagonal components of the Green's functions can be expressed in terms of the density of states $\rho_j(\omega)$ in such a way that

$$\text{Im}[G_{d,M}^R]_{jj}(\omega) = -\pi\hbar\rho_j(\omega) \quad (\text{S40a})$$

$$\text{Re}[G_{d,M}^R]_{jj}(\omega) = \frac{1}{\pi}\mathcal{P} \int d\omega' \frac{\text{Im}[G_{d,M}^R]_{jj}(\omega')}{\omega' - \omega} = -\mathcal{P} \int d\epsilon' \frac{\rho_j(\omega')}{\omega' - \omega}. \quad (\text{S40b})$$

At resonance, the density of states becomes of the Lorentzian form:

$$\rho_j(\omega) = \frac{1}{\pi\hbar} \frac{\Gamma_j/2}{\omega^2 + (\Gamma_j/2)^2}. \quad (\text{S41})$$

The admittance at resonance can be simplified into

$$g(\omega) = \frac{\hbar\omega}{R_Q} \left[i\mathcal{P} \int \int \frac{d\epsilon' d\epsilon''}{\epsilon'' - \epsilon'} (f(\epsilon' - \hbar\omega) - f(\epsilon'')) \rho_1(\omega - \omega') \rho_2(\omega'') \right. \\ \left. + \pi \int d\epsilon' (f(\epsilon' - \hbar\omega) - f(\epsilon')) \rho_1(\omega - \omega') \rho_2(\omega') \right] \quad (\text{S42})$$

with $\epsilon' = \hbar\omega'$ and $\epsilon'' = \hbar\omega''$ and \mathcal{P} meaning the principal value. At zero temperature, it is further simplified into

$$g(\omega) = \frac{\hbar\omega}{R_Q} \left[\pi \int_0^{\hbar\omega} d\epsilon' \rho_1(\omega - \omega') \rho_2(\omega') + i\mathcal{P} \int_{-\infty}^0 d\epsilon' \int_0^{\infty} d\epsilon'' \frac{2(\epsilon'' - \epsilon')}{(\epsilon'' - \epsilon')^2 - (\hbar\omega)^2} \rho_1(\omega') \rho_2(\omega'') \right], \quad (\text{S43})$$

justifying Eq. (12) in the main text.

E. Relaxation Resistance at Finite Temperatures: Sommerfeld Expansion

It is difficult to obtain an analytical expression for finite-temperature resistance. However, the low-temperature behavior can be examined by using the Sommerfeld expansion, which expands the integral as

$$\int d\epsilon f(\epsilon) h(\epsilon) = \int_{-\infty}^0 d\epsilon h(\epsilon) + \sum_{n=1}^{\infty} \alpha_{2n} (k_B T)^{2n} h^{(2n-1)}(0), \quad (\text{S44})$$

where $\alpha_{2n} = 2\zeta(2n)(1 - 2^{1-2n})$. Then, up to the second order in $k_B T$, one obtains

$$g(\omega) \approx g(\omega)|_{T=0}$$

$$-\frac{1}{R_Q} \left(\frac{k_B T}{\hbar} \right)^2 \frac{\pi^2}{6} \left[\sum_{\mu} \left(\frac{\Gamma_+}{\Gamma_+ + i\omega} + \frac{\Gamma_-^2}{\varepsilon(\varepsilon - \mu\omega)} \right) \left(\frac{1}{(\omega - i\Gamma_+/2 - \mu\varepsilon/2)^2} - \frac{1}{(i\Gamma_+/2 + \mu\varepsilon/2)^2} \right) \right. \\ \left. + \frac{2\Gamma_-^2\omega}{\varepsilon(\varepsilon^2 - \omega^2)} \left(\frac{1}{(i\Gamma_+/2 + \varepsilon/2)^2} - \frac{1}{(i\Gamma_+/2 - \varepsilon/2)^2} \right) \right]. \quad (\text{S45})$$

For the Dirac fermion edge mode ($\Gamma_1 = \Gamma_2$), the zero-frequency resistance at low temperatures is then given by

$$R_0 = \frac{R_Q}{2} \left[1 + \frac{4\pi^2}{3} \left(\frac{k_B T}{\varepsilon_d} \right)^2 \left(\frac{(\varepsilon_d/\hbar)^2}{(\varepsilon_d/\hbar)^2 + (\Gamma_+/2)^2} \right)^2 \right]. \quad (\text{S46})$$

On the other hand, in the cTSC₁ phase ($\Gamma_2 = 0$), the Sommerfeld expansion of R_0 is expressed as

$$R_0 = R_Q \left(\frac{k_B T}{\varepsilon_d} \right)^2 \frac{4\pi^2}{3} \left(\frac{(\varepsilon_d/\hbar)^2 - \Gamma_+^2}{(\varepsilon_d/\hbar)^2} \right)^2 \left(1 - i \frac{\Gamma_+}{\varepsilon} \ln \frac{\Gamma_+ - i\varepsilon}{\Gamma_+ + i\varepsilon} \right)^{-2}. \quad (\text{S47})$$

Note that the stark contrast between two cases at the resonance ($\varepsilon_d = 0$): In the QAH phase the second-order term vanishes, indicating some immunity to thermal fluctuations, while R_0 diverges in the cTSC₁ phase. Surely the above expansion for the case of a single Majorana fermion edge mode is valid only for $k_B T \ll \hbar\Gamma_m$ so the $\varepsilon_d \rightarrow 0$ limit cannot be taken from it. But still the non-monotonic behavior or the increase of the resistance at finite temperatures, discussed in the main text, are qualitatively captured in this expansion. In the case of weak-coupling limit ($|\varepsilon_d/\hbar| \gg \Gamma_1$), the expansion leads to Eq. (13).

III. COMPARISON WITH THE CASE WITH ANDREEV EDGE MODES

A. Andreev Edge Modes: Conventional Andreev Edge Mode vs. Majorana Mode

Majorana Fermion edge mode is a special case of ‘‘Andreev edge modes,’’ i.e., the Andreev bound states localized at (yet propagating along) the edge of the superconducting film. Suppose either that the superconducting order parameter is suppressed close to the edge of the superconducting film or that a thin conducting wire is in contact with the superconducting film [see Fig. S1(a)]. In either case, there forms a superconductor-normal junction between the superconducting region and the thin normal conducting region. As quasi-particles with energy lower than the superconducting gap Δ cannot penetrate into the superconducting region, they are confined in the normal region [10–12], forming a one-dimensional mode

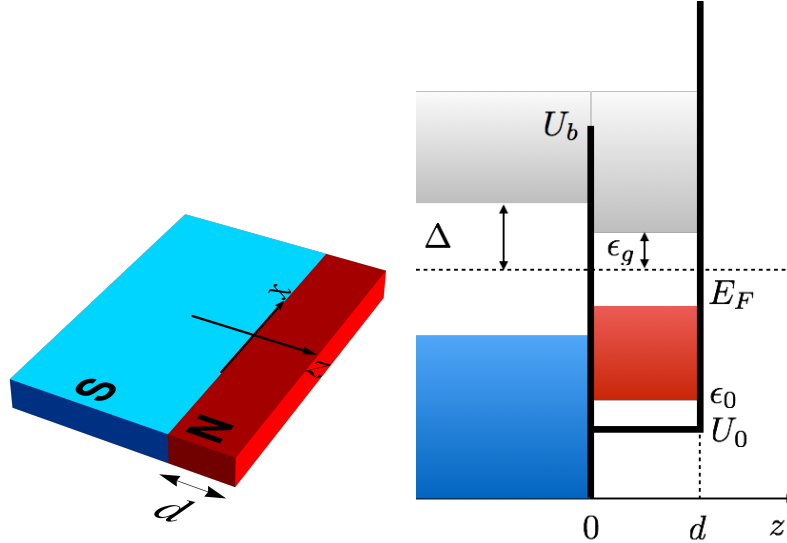


FIG. S1. (a) Superconductor-normal junction between superconducting thin film and a thin conducting wire. (b) Schematic energy configuration of the system on (a).

propagating along the edge direction. When the superconducting state is topologically non-trivial, the Andreev edge mode has the Majorana fermion character protected against local fluctuations and disorders (see, e.g., [13, 14]).

With regard to the charge relaxation resistance, all Andreev edge modes (irrespective of whether they are Majorana or not) have one important common property: As they originate from the Andreev reflection at the superconductor-normal interface, they are mixtures of particles and holes with comparable amplitudes. However, Majorana edge modes have two distinguished differences compared with conventional Andreev states: First, Majorana edge mode is gapless while conventional Andreev edge mode has a finite excitation gap. Second, Majorana mode is “real” and only a half of Dirac fermion while Andreev edge mode consists of usual Dirac fermion. In this section, we examine the effects of the similarity and differences on the charge relaxation resistance in a quantum capacitor-resistor circuit.

B. Model for Conventional Andreev Edge Mode

We follow Ref. [12] to consider a simplest possible model for a conventional Andreev edge mode. We assume an s -wave superconductor and the normal conductor is a semiconducting nanowire in the ballistic regime. The latter assumption is to avoid disorder effect, which is certainly interesting on its own but out of scope of the current work. As shown in detail in [12], the Andreev states bound in the normal region is effectively described by the proximity-induced pairing potential Δ_{ind} . Namely, the dispersion relation of

the Andreev states is given by

$$\epsilon_k = \sqrt{\Delta_{\text{ind}}^2 + (\xi_k - \delta\mu)^2}, \quad (\text{S48})$$

where $\xi_k \equiv \hbar^2 k^2 / 2m - E_F$ (with k being the momentum along the edge direction) is the kinetic energy relative to the Fermi level and $\delta\mu$ is additional shift in the chemical potential. To compare with the case of Majorana states, we further assume low transparency of the interface between the superconducting and normal region, where $\Delta_{\text{ind}}, \delta\mu \ll \Delta$. Therefore, the Hamiltonian for the lead [to be compared with Eqs. (1), (5) and (7a) in the main text] is given by

$$H_{\text{Andreev}} = \sum_{k\sigma} \epsilon_k b_{k\sigma}^\dagger b_{k\sigma} \quad (\text{S49})$$

where $b_{k\sigma}$ is the Bogoliubov quasi-particle operator with spin σ and momentum k along the edge. The tunneling Hamiltonian [to be compared with Eqs. (3), (6) and (7b) in the main text] reads as

$$H_{\text{tun}} = t \sum_{k\sigma} \left[\text{sign}(\sigma) A_k^* b_{k\sigma}^\dagger + B_k b_{k\bar{\sigma}} \right] d_{k\sigma} + h.c. \quad (\text{S50})$$

where $\bar{\sigma}$ means the spin direction opposite to σ . Here A_k and B_k are proportional to the proximity-induced BCS coherence factors [15]

$$A_k \propto \sqrt{\frac{1}{2} \left[1 + \frac{(\xi_k - \delta\mu)}{\Delta_{\text{ind}}} \right]}, \quad B_k \propto \sqrt{\frac{1}{2} \left[1 - \frac{(\xi_k - \delta\mu)}{\Delta_{\text{ind}}} \right]}. \quad (\text{S51})$$

Essentially, A_k (B_k) is responsible for single-electron (pair) tunneling process. We note that there is additional momentum dependence of the relative strength of the amplitudes, A_k and B_k , of the two processes ($A_k \approx B_k$ for $k = k_F$) while in Eq. (6) in the main text the relative strength, $t_{\text{single}}/t_{\text{pair}}$, is momentum independent (except for weak dependence depending on the system details).

A remark is in order: To compare with the case with Majorana modes, we have to consider spinful level on the quantum dot. It is because if the quantum dot is spin polarized, then the single-particle and pair tunneling process involves the distinct modes of opposite spins and the feature of particle-hole mixture in the Andreev states does not play any role.

C. Linear Response Theory

Now we apply the linear response theory, following the exactly same procedure as in the previous sections, to the s -wave Andreev edge modes in order to obtain the admittance through the quantum dot which is now coupled to the Andreev modes. Since the structure of Hamiltonians, Eqs. (S49) and (S50) is basically identical to that of Eqs. (5) and (6) in the text, respectively, the linear response theory results in the

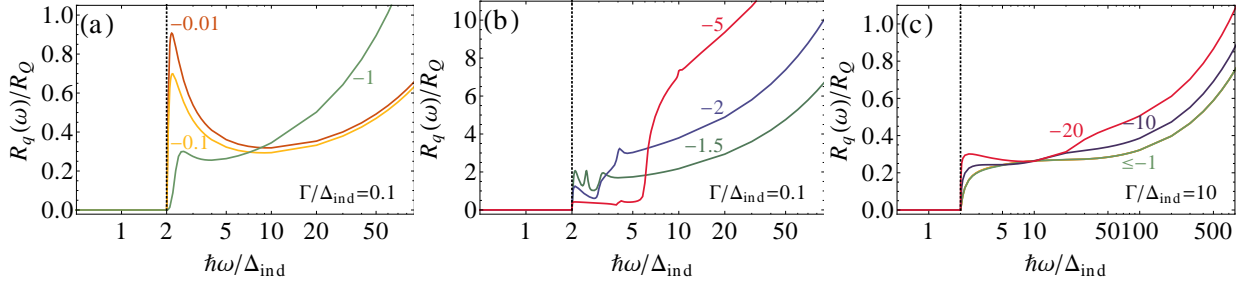


FIG. S2. Zero-temperature resistance $R_q(\omega)$ as a function of frequency ω for (a,b) the weak-coupling case ($\Gamma/\Delta_{\text{ind}} = 0.1$) and (c) the strong-coupling case ($\Gamma/\Delta_{\text{ind}} = 10$). Each curve corresponds to different value of $\epsilon_d/\Delta_{\text{ind}}$ which is annotated in the figure. The dotted lines indicates the minimal energy of p-h pairs, $\hbar\omega = 2\Delta_{\text{ind}}$.

same expression for the admittance as given in Eq. (S28) except two points. First, an additional factor 2 is multiplied. It is because we are considering the s -wave superconductor which has two degenerate spins. Each of spin channels makes the same contribution so that the admittance is doubled compared to the spin-polarized p -wave case. Second, since the QD-edge mode tunneling is inevitably momentum-dependent via the coefficients A_k and B_k , the self energy for the QD Green's function

$$G_d^{R/A}(t, t') = \mp i\Theta(\pm(t - t')) \begin{bmatrix} \langle |\{d_\uparrow(t), d_\uparrow^\dagger(t')\}| \rangle & \langle |\{d_\downarrow(t), d_\uparrow^\dagger(t')\}| \rangle \\ \langle |\{d_\uparrow^\dagger(t), d_\downarrow^\dagger(t')\}| \rangle & \langle |\{d_\downarrow^\dagger(t), d_\downarrow^\dagger(t')\}| \rangle \end{bmatrix} \quad (\text{S52})$$

is now also energy-dependent:

$$\Sigma^{R/A}(\omega') = \frac{\Gamma}{2} \frac{\omega' \sigma_0 - (\Delta_{\text{ind}}/\hbar) \sigma_1}{i\sqrt{(\omega' \pm i\eta)^2 - (\Delta_{\text{ind}}/\hbar)^2}} \quad (\text{S53})$$

with

$$\sqrt{(\omega' \pm i\eta)^2 - (\Delta_{\text{ind}}/\hbar)^2} = \begin{cases} i\sqrt{(\Delta_{\text{ind}}/\hbar)^2 - \omega'^2}, & \Delta_{\text{ind}} > \hbar|\omega'| \\ \pm \text{sign } \omega' \sqrt{\omega'^2 - (\Delta_{\text{ind}}/\hbar)^2}, & \Delta_{\text{ind}} < \hbar|\omega'|. \end{cases} \quad (\text{S54})$$

Here, in obtaining the self energy, we have assumed for simplicity that the effective Fermi level is high enough that the dispersion relation $\xi_k - \delta\mu$ around the Fermi level is well linearized. The relaxation resistance $R_q(\omega) = \text{Re}[1/g(\omega)]$ is then obtained by numerically integrating Eq. (S28) with the self energy, Eq. (S53).

D. Relaxation Resistance: Below the Superconducting Gap

Here we focus on the zero temperature case ($k_B T = 0$). Figure S2 displays the resistance $R_q(\omega)$ as a function of frequency ω for the weak- and strong-coupling cases for several values of ϵ_d . First, consider the

frequency ω smaller than $2\Delta_{\text{ind}}$. In this region, the zero-temperature resistance $R_q(\omega)$ vanishes completely, independent of the strength of the QD-reservoir coupling. This is consistent with our previous argument based on the p-h pairs: No p-h pair with the energy less than $2\Delta_{\text{ind}}$ cannot be generated due to the (induced) superconducting gap so the resistance for the frequency below $2\Delta_{\text{ind}}$ is zero. At finite temperatures, the thermal fluctuations will relax this energy conservation constraint, giving rise to finite $R_q(\omega)$ for $\hbar|\omega| < \Delta_{\text{ind}}$. However, the resistance should be still exponentially small if $k_B T \ll \Delta_{\text{ind}}$. This is one of main differences distinguishing between the Majorana fermions and the ordinary Andreev modes.

It should be also noted that the resistance at $\hbar\omega = 2\Delta_{\text{ind}}$ is still zero. It might look unphysical considering that the density of states (DOS) is divergent at the superconducting gap: The large DOS is expected to enhance the generation of p-h pairs with the energy $2\Delta_{\text{ind}}$. However, at this energy, $A_k = B_k$ so that the destructive interference between the single-electron and pair tunneling processes, discussed in the text, is maximal so that the resistance vanishes. For the Majorana fermion case, it happens at zero frequency, while it is moved to $2\Delta_{\text{ind}}$ for the *s*-wave Andreev modes. It also explains a rather rapid increases of $R_q(\omega)$ with increasing ω just beyond $2\Delta_{\text{ind}}$. The increase in $R_q(\omega)$ results from the still large DOS and the gradual lift of the destructive interference condition ($A_k \neq B_k$).

E. Relaxation Resistance: Above the Superconducting Gap

Now we turn to the relaxation resistance $R_q(\omega)$ at high frequencies: $\omega \geq 2\Delta_{\text{ind}}$. It behaves differently depending on the coupling strength. We examine two representative cases; first the weak-coupling case ($\Gamma/\Delta_{\text{ind}} = 0.1$) and later the strong coupling case ($\Gamma/\Delta_{\text{ind}} = 10$). In the weak-coupling case, as mentioned above, there is a rather rapid increase in $R_q(\omega)$ just beyond $2\Delta_{\text{ind}}$, which forms a peak or a cusp near $\hbar\omega = 2\Delta_{\text{ind}}$, depending on the value of ϵ_d . For $|\epsilon_d| \leq \Delta_{\text{ind}}$, that is, when the QD level is inside the superconducting gap, there exists no other feature than a monotonic increase of $R_q(\omega)$ with increasing ω beyond $2\Delta_{\text{ind}}$ [see Fig. S2(a)]. In addition, the peak height near $\hbar\omega = 2\Delta_{\text{ind}}$ decreases as ϵ_d approaches the gap boundary. Once the QD level ϵ_d goes out of the gap, additional features arise: see Fig. S2(b). Additional enhancement of the resistance is observed at $\hbar\omega = |\epsilon_d| + \Delta_{\text{ind}}$ ($> 2\Delta_{\text{ind}}$) and $2|\epsilon_d|$ ($> 2\Delta_{\text{ind}}$), at which additional peaks or cusps in $R_q(\omega)$ are formed. At these frequencies the p-h pair generation is assisted by the resonance between the QD level and the superconducting quasi-particle. The resonance can also affect the peak near $\hbar\omega = 2\Delta_{\text{ind}}$ if $|\epsilon_d| \gtrsim \Delta_{\text{ind}}$: see $\epsilon_d/\Delta_{\text{ind}} = -1.5$ case in Fig. S2(b). It is the result of the interplay between the QD resonance and the large DOS near the gap boundary. Therefore, the height of the peak near $\hbar\omega = 2\Delta_{\text{ind}}$ rapidly surges at $|\epsilon_d| \approx \Delta_{\text{ind}}$ and then decreases again with increasing $|\epsilon_d|$.

Before discussing the strong-coupling case, we summarize the differences in the finite-frequency behav-

ior of $R_q(\omega)$ for the Andreev edge modes and for the Majorana edge modes. While in both cases $R_q(\omega)$ varies non-monotonically with frequency, the dependence of the peak/cusp position on the QD level ϵ_d exhibits a clear difference: In the Majorana fermion case, the peak position scales with $\Gamma_m \propto \epsilon_d^2$, while in the Andreev mode case the peaks are pinned at $2\Delta_{\text{ind}}$ or have a linear dependence on ϵ_d . Also, while in the former case the peak height increases monotonically with decreasing $|\epsilon_d|$ or as approaching the resonance [see Fig. 4(b)], in the latter case the peak height varies non-monotonically with ϵ_d since the finite gap $2\Delta_{\text{ind}}$ is introduced.

Finally, the strong-coupling case ($\Gamma/\Delta_{\text{ind}} = 10$) is examined [see Fig. S2(c)]. The strong tunneling smears out the peak/cusp structures by widening the QD level. Hence, no special feature remains. The resistance remains small for low frequencies, no matter what values ϵ_d has: Fig. S2(c) shows that $R_q(\omega) \rightarrow R_Q/4 \neq 0$ (here $R_Q/4$ rather than $R_Q/2$ because of two spin components) as $\omega \rightarrow 0$ (keeping $\omega > \Delta_{\text{ind}}$). In real experiments, Δ_{ind} might be so small that typical samples might have $\Gamma > \Delta_{\text{ind}}$. Our results show that even in this case the Majorana fermion reservoir (having a vanishingly small gap) and the Andreev edge modes (having a finite but small gap) exhibit distinctive behavior of $R_q(\omega)$ with respect to the frequency and the QD level.

F. Summary of Differences between s -wave Andreev Edge Mode and Majorana Mode

Here we summarize the major differences between s -wave Andreev edge mode and Majorana mode:

1. $R_q(\omega) = 0$ *identically* for all $0 < \omega \leq 2\Delta_{\text{ind}}$ in the Andreev case while $R_q(\omega) \propto \omega^2$ as $\omega \rightarrow 0$ in the Majorana case.
 - (a) For large gap ($\Delta_{\text{ind}} \gg \Gamma_1$), this difference is evident.
 - (b) For small gap ($\Delta_{\text{ind}} \ll \Gamma_1$), where the gap is difficult to resolve experimentally, $R_q(\omega) \rightarrow R_Q/4 \neq 0$ (here $R_Q/4$ rather than $R_Q/2$ because of two spin components) as $\omega \rightarrow 0$ (keeping $\omega > \Delta_{\text{ind}}$) in the Andreev case. This is shown in Fig. S2(c) and in contrast with $\lim_{\omega \rightarrow 0} R_q(\omega) \rightarrow 0$ in the Majorana case.
2. $R_q(\omega)$ at higher frequencies may be non-monotonic for both cases. However, the peak positions behave distinctively:
 - (a) In the Majorana case, the peaks are at $\omega \approx \Gamma_m = 4\epsilon_d^2/\Gamma_1$. This is shown in Fig. S2(b).
 - (b) In the Andreev case with $\Delta_{\text{ind}} \gg \Gamma_1$, the peaks are at $\omega \approx 2\Delta_{\text{ind}}$. There may be additional peaks at $\omega \approx \Delta_{\text{ind}} + |\epsilon_d|$ when $|\epsilon_d| > \Delta_{\text{ind}}$. This is shown in Figs. S2(a) and (b).

(c) In the Andreev case with $\Delta_{\text{ind}} \ll \Gamma_1$, $R_q(\omega)$ is almost monotonic and independent of ϵ_d . This is shown in Fig. S2(c).

In conclusion, the Majorana fermion reservoir is well distinguished from the *s*-wave Andreev edge modes in the frequency- and QD-level-dependence of $R_q(\omega)$. So the ac response can be used to detect the existence of the Majorana fermions unambiguously.

-
- [1] X.-L. Qi, T. L. Hughes, and S.-C. Zhang, *Phys. Rev. B* **82**, 184516 (2010).
 - [2] R. Žitko, *Phys. Rev. B* **83**, 195137 (2011).
 - [3] M. Büttiker, H. Thomas, and A. Prêtre, *Phys. Lett. A* **180**, 364 (1993).
 - [4] M. Büttiker, A. Prêtre, and H. Thomas, *Phys. Rev. Lett.* **70**, 4114 (1993).
 - [5] S. Nigg, R. López, and M. Büttiker, *Phys. Rev. Lett.* **97**, 206804 (2006).
 - [6] M. Lee, R. López, M.-S. Choi, T. Jonckheere, and T. Martin, *Phys. Rev. B* **83**, 201304 (2011).
 - [7] H. Khim, S.-Y. Hwang, and M. Lee, *Phys. Rev. B* **87**, 115312 (2013).
 - [8] N. Wingreen, A.-P. Jauho, and Y. Meir, *Phys. Rev. B* **48**, 8487 (1993).
 - [9] A.-P. Jauho, N. Wingreen, and Y. Meir, *Phys. Rev. B* **50**, 5528 (1994).
 - [10] A. F. Andreev, *Sov. Phys. JETP* **22**, 455 (1966).
 - [11] A. V. Shytov, P. A. Lee, and L. S. Levitov, *Physics-Uspekhi* **41**, 207 (1998).
 - [12] A. F. Volkov, P. H. C. Magnée, B. J. van Wees, and T. M. Klapwijk, *Physica C* **242**, 261 (1995).
 - [13] N. Read and D. Green, *Phys. Rev. B* **61**, 10267 (2000).
 - [14] M. Sato and S. Fujimoto, *Phys. Rev. B* **79**, 094504 (2009).
 - [15] P. G. de Gennes, *Superconductivity of Metals and Alloys* (Westview Press, New York, 1999).